Electronic Supplementary Material (ESI) for Dalton Transactions.
This journal is © The Royal Society of Chemistry 2018

Supplementary information to:

Rapid Water Disinfection over Ag/AgBr/Covalent Triazine-Based Framework Composite under Visible Light

Liuyi Li,[ac] Xiaofen Li,[b] Zhi Cheng,[b] Jinhong Bi,[*ab] Shijing Liang,[ab] Zizhong Zhang,[a]
Yan Yu,[c] Ling Wu[*a]

a Dr. L. Li, Prof. J. Bi, Dr. S. Liang, Prof. Z. Zhang, Prof. L. Wu
State Key Laboratory of Photocatalysis on Energy and Environment, Fuzhou University, Minhou, Fujian 350002, P. R. China.
E-mail: bijinhong@fzu.edu.cn; wuling@fzu.edu.cn
b Ms. X. Li, Ms. Z. Cheng, Dr. S. Liang, Prof. J. Bi
Department of Environmental Science and Engineering, Fuzhou University, Minhou, Fuzhou 350108, P. R. China.
c Dr. L. Li, Prof. Y. Yu
Key Laboratory of Eco-materials Advanced Technology, College of Materials Science and Engineering, Fuzhou University, Minhou, Fuzhou 350108, P. R. China

General information. Trifluoromethanesulfonic acid (99%) and terephthalonitrile (98%) were purchased from Adamas-beta. Hexadecyl trimethyl ammonium bromide (CTAB), silver nitrate ($AgNO_3$), dichloromethane, ammonia solution, methanol and sodium chloride (NaCl) were purchased from Sinopharm Chemical Reagent Co., Ltd. All reagents were of analytical grade and directly used as received without further purification. Deionized water with a resistivity of 18.25 MΩ·cm was used throughout the experiments. Powder X-ray diffraction (XRD) was performed to investigate the crystal structure of the samples on a Rigaku MiniFlex 600 X-ray diffractometer with Ni- filtered Cu Kα irradiation (α=1.5406 Å). And data were recorded at a scan rate of 0.8 sec/step in the range from 5^{o} to 80^{o}. Fourier transform infrared (FT-IR) spectra of the samples were recorded on a Thermo Scientific Nicolet iS10 spectrometer by using KBr pellets. Nitrogen adsorption-desorption isotherm measurements on a micromeritics ASAP-2020 HD88 system were carried out to investigate the Brunauer-Emmett-Teller (BET) surface area of the samples. Morphology of the as-prepared samples was observed via transmission electron microscopy (TEM) with a JEOL model JEM 2010 EX instrument and scanning electron microscopy (SEM) with a FEI Nova NANO-SEM 230 spectrophotometer. UV-vis diffuse reflectance spectra (DRS) of the samples were recorded between the range 200 and 800 nm on a Varian Cary 500 Scan UV-vis-NIR spectrometer, using $BaSO_4$ as the background. Raman spectra of the samples were obtained using 325 nm lasers on a Renishaw inVia system. X-ray photoelectron spectroscopy (XPS) measurement was conducted on a VG Scientific ESCA Lab Mark II spectrometer equipped with two ultra-high vacuum 6 (UHV) chambers. The binding energies of all tested samples were referenced to the C1s peak (284.6 eV) of the surface adventitious carbon. Inductively Coupled Plasma-Optical Emission Spectrometer (ICP-OES) (Optima 7000DV) was carried out to determine the amount of Ag^+. The amount of H_2O_2 was determined on a Hitachi F-4500 fluorescence spectrophotometer based on the reaction of H_2O_2 with courmarin to form a high fluorescent compound (7-hydroxylcoumarin, 456 nm). The zeta potential measurements were carried out on PALS Zeta Potential Measurement in the presence of aqueous solution at different pH values (NanoBrook Omni, Brookhaven, American). In this case, the suspension of 4 mL deionized water containing 1 mg of the samples were prepared, respectively. The required pH value was adjusted by adding an appropriate amount of 0.01 M HCl solution or 0.01 M NaOH solution. Each average value was the result of three repetitions.

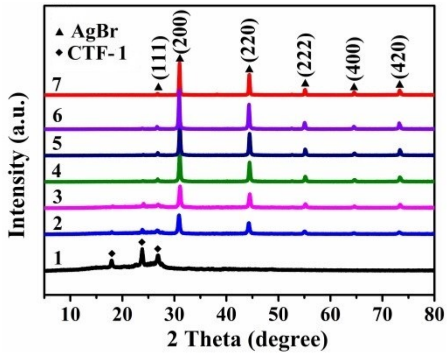

Figure S1. XRD patterns of the as-prepared series samples: (1) CTF-1, (2) Ag/AgBr/CTF-10, (3) Ag/AgBr/CTF-30, (4) AgBr/AgBr/CTF-50, (5) Ag/AgBr/CTF-70, (6) Ag/AgBr/CTF-90 and (7) Ag/AgBr.

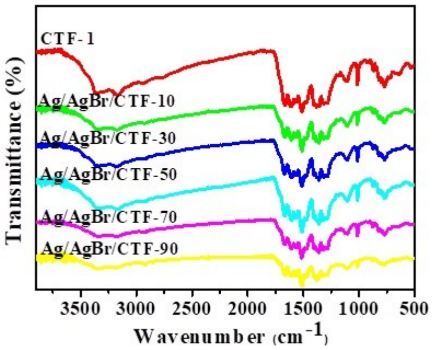

Figure S2. FT-IR spectra of the as-prepared CTF-1 and Ag/AgBr/CTFs composites.

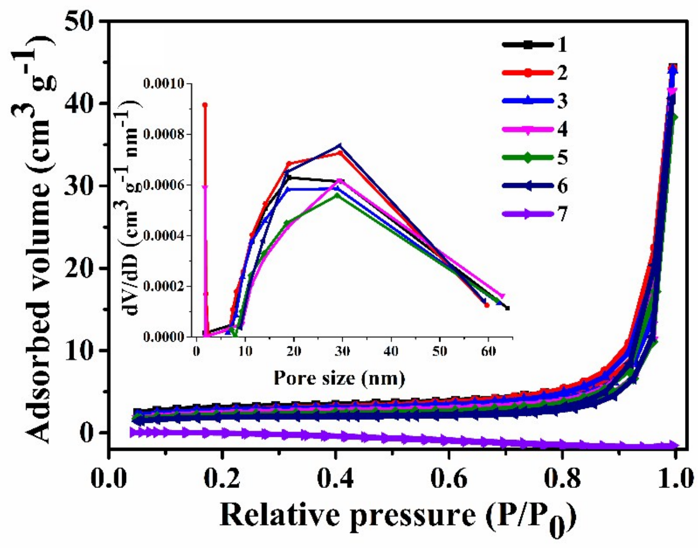

Figure S3. N_2 adsorption-desorption isotherms and pore structure of the as-prepared series samples: (1) CTF-1, (2) Ag/AgBr/CTF-10, (3) Ag/AgBr/CTF-30, (4) AgBr/AgBr/CTF-50, (5) Ag/AgBr/CTF-70, (6) Ag/AgBr/CTF-90 and (7) Ag/AgBr.

Table S1 Specific surface area, pore volume, and pore size of the as-prepared CTF-1, Ag/AgBr/CTFs and Ag/AgBr series samples.

Sample	Surface area (m^2/g)	Pore volume (cm^3/g)	Average pore size (nm)
CTF-1	9.3	0.07	29.6
Ag/AgBr/CTF-10	9.4	0.07	29.0
Ag/AgBr/CTF-30	8.6	0.07	31.9
Ag/AgBr/CTF-50	7.3	0.06	35.2
Ag/AgBr/CTF-70	6.8	0.06	34.8
Ag/AgBr/CTF-90	6.0	0.06	40.9
Ag/AgBr	0.04	-	-

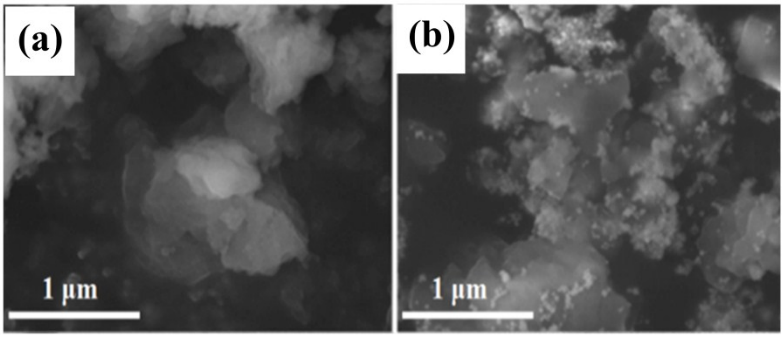

Figure S4. SEM image of CTF-1 (a) and Ag/AgBr/CTF-50 (b).

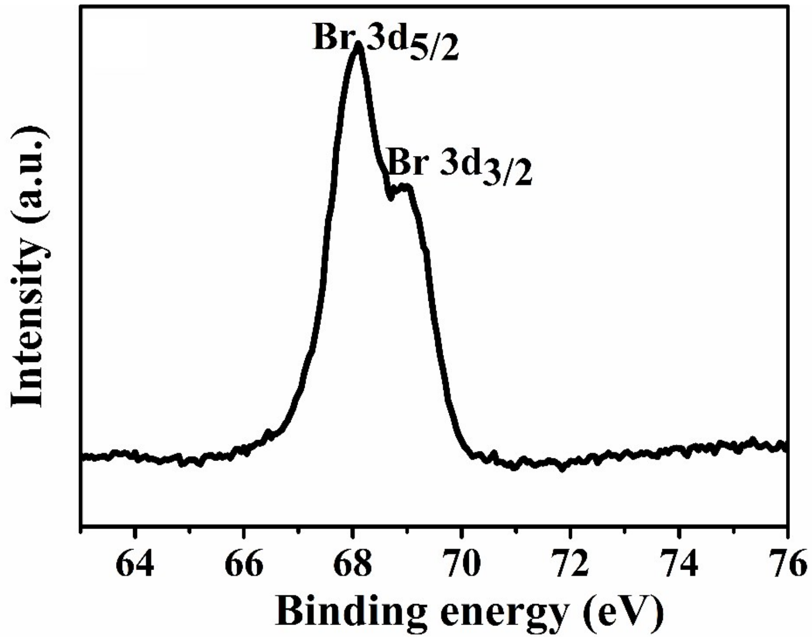

Figure S5. Br 3d XPS spectra of Ag/AgBr/CTF-50.

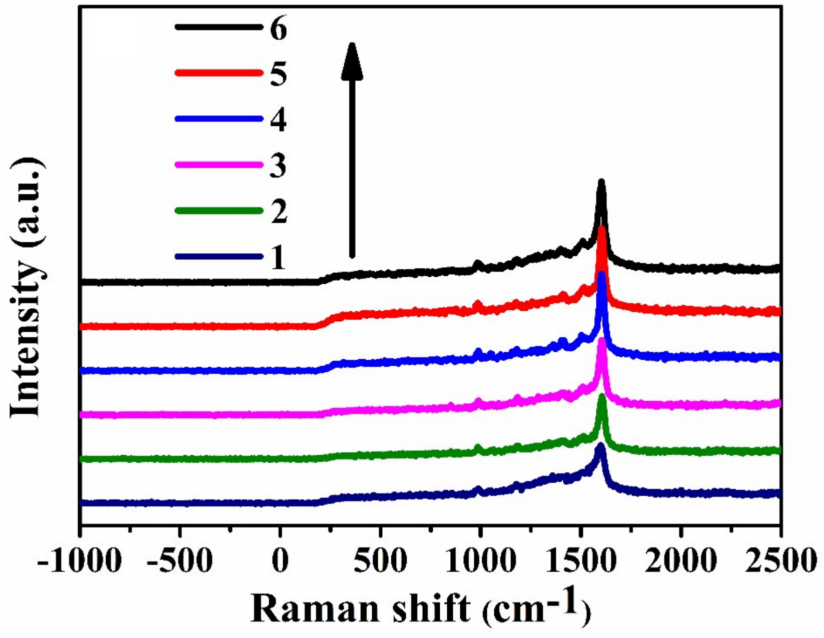

Figure S6. Raman spectra of Ag/AgBr/CTF-1 series samples: (1) CTF-1, (2) Ag/AgBr/CTF-10, (3) Ag/AgBr/CTF-30, (4) AgBr/AgBr/CTF-50, (5) Ag/AgBr/CTF-70 and (6) Ag/AgBr/CTF-90.

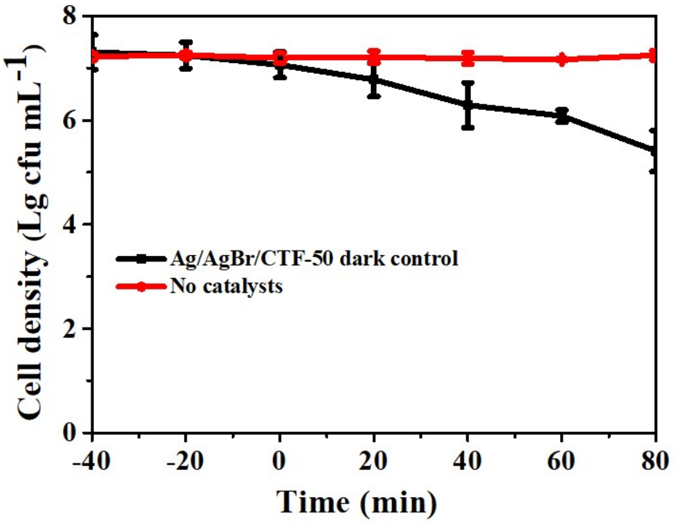

Figure S7. Photocatalytic inactivation efficiencies of *E. coli* in light control and dark control experiments.

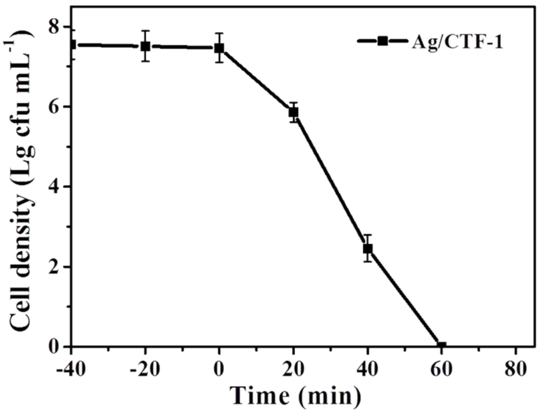

Figure S8. Photocatalytic inactivation efficiency of *E. coli* under visible light irradiation by Ag/CTF-1.

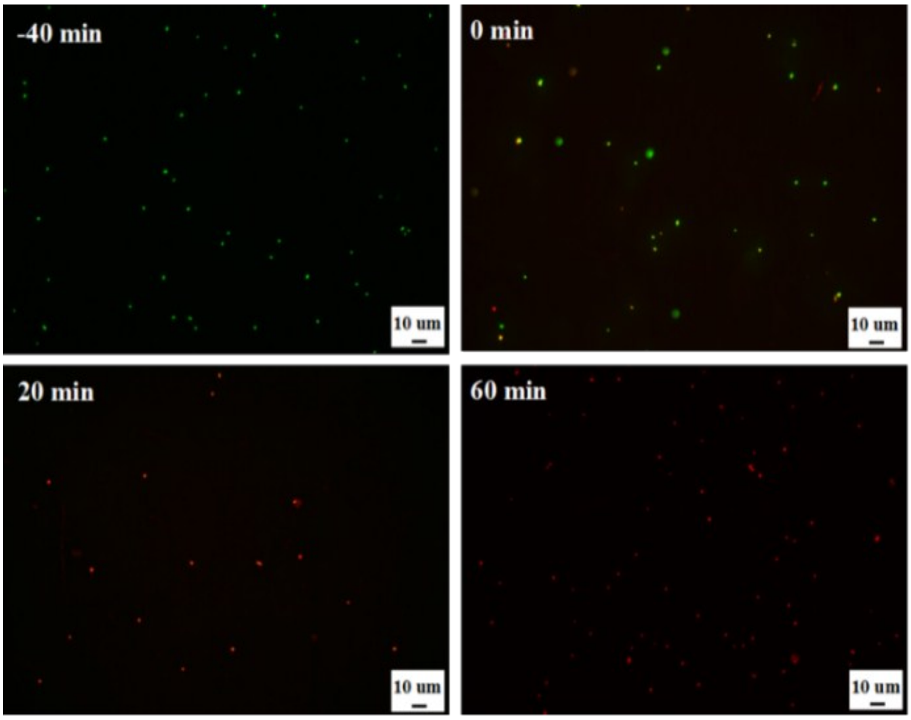

Figure S9. Fluorescence microscopic images of *E. coli* photocatalytically treated with Ag/AgBr/CTF-50 under visible light irradiation in different time.

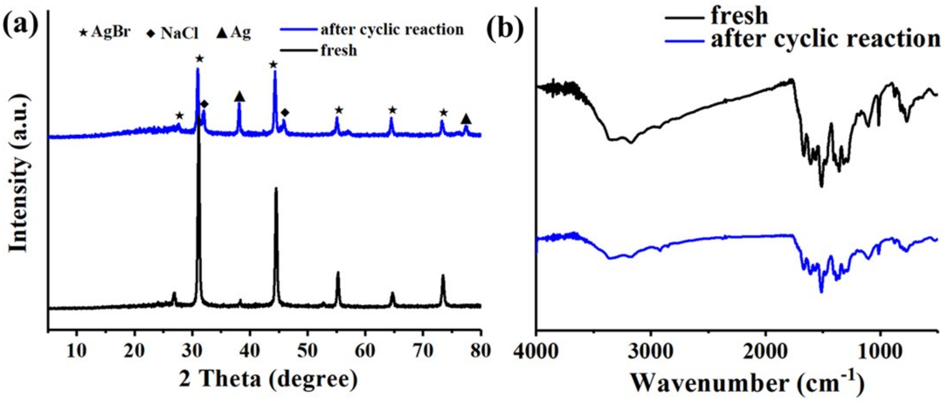

Figure S10. XRD patterns and FTIR spectra of Ag/AgBr/CTF-50 before and after cyclic reaction.

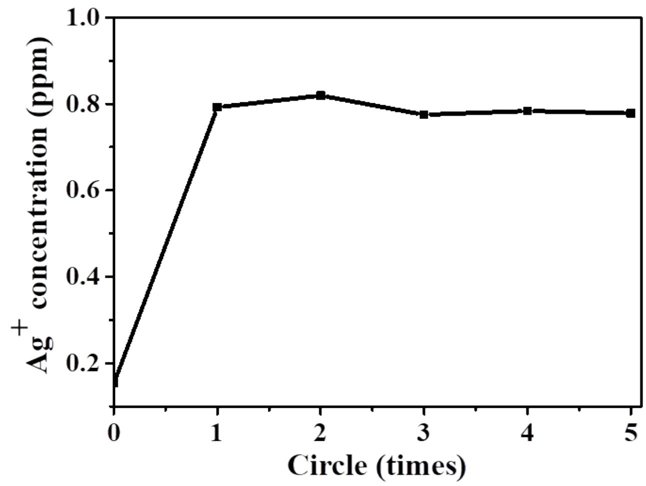

Figure S11. The concentration of the eluted Ag$^+$ determined by ICP-OES during five cycling process.

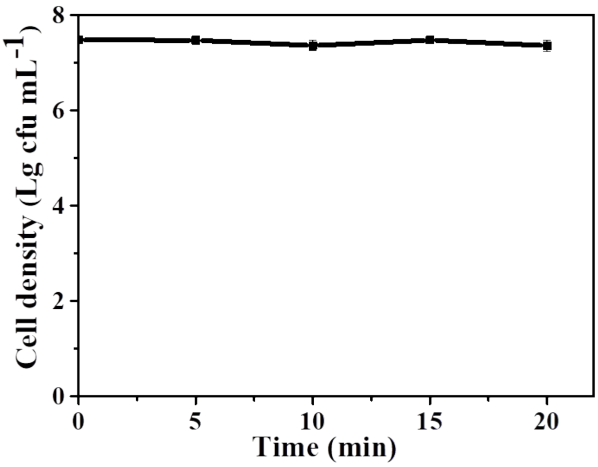

Figure S12. Photocatalytic inactivation efficiency of *E. coli* K-12 under visible light irradiation using 0.82 ppm Ag$^+$ solution.

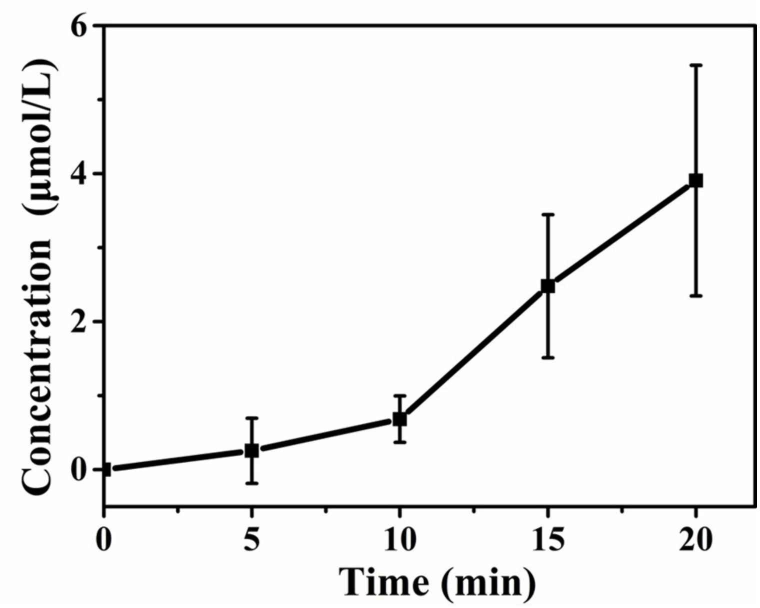

Figure S13. Accumulation of H_2O_2 produced in the presence of Ag/AgBr/CTF-50 under visible-light irradiation.

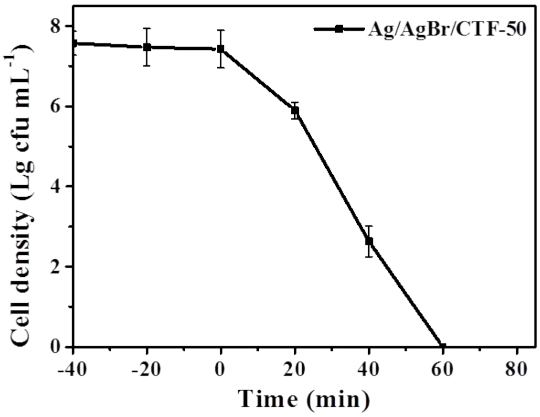

Figure S14. Photocatalytic inactivation efficiency of *E. coli* under 450nm cutoff filter by using Ag/AgBr/CTF-50.

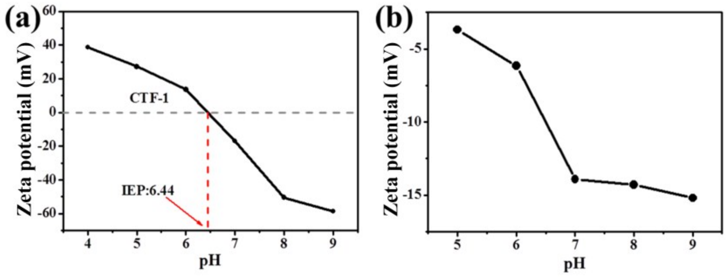

Figure S15. Zeta potential of CTF-1(a) and *E. coli* (b) in aqueous solution.